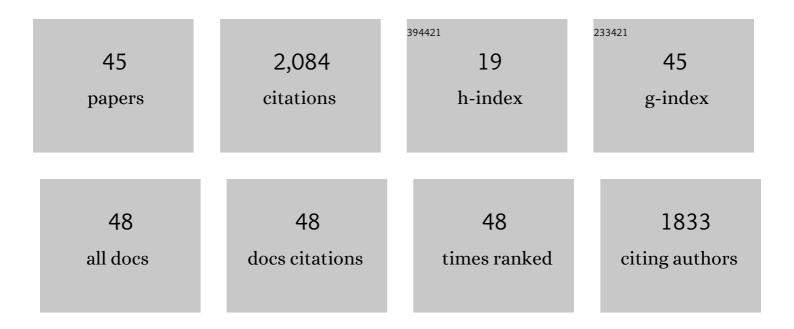
Chu-Ting Yang

List of Publications by Year in descending order

Source: https://exaly.com/author-pdf/5771398/publications.pdf Version: 2024-02-01



#	Article	IF	CITATIONS
1	Alkylboronic Esters from Copperâ€Catalyzed Borylation of Primary and Secondary Alkyl Halides and Pseudohalides. Angewandte Chemie - International Edition, 2012, 51, 528-532.	13.8	360
2	Copper atalyzed Cross oupling Reaction of Organoboron Compounds with Primary Alkyl Halides and Pseudohalides. Angewandte Chemie - International Edition, 2011, 50, 3904-3907.	13.8	194
3	Copper-Catalyzed Cross-Coupling of Nonactivated Secondary Alkyl Halides and Tosylates with Secondary Alkyl Grignard Reagents. Journal of the American Chemical Society, 2012, 134, 11124-11127.	13.7	178
4	Roomâ€Temperature Copper atalyzed Carbon–Nitrogen Coupling of Aryl lodides and Bromides Promoted by Organic Ionic Bases. Angewandte Chemie - International Edition, 2009, 48, 7398-7401.	13.8	165
5	Copper-Catalyzed/Promoted Cross-coupling of <i>gem</i> -Diborylalkanes with Nonactivated Primary Alkyl Halides: An Alternative Route to Alkylboronic Esters. Organic Letters, 2014, 16, 6342-6345.	4.6	147
6	Alkylboronic Esters from Palladium―and Nickelâ€Catalyzed Borylation of Primary and Secondary Alkyl Bromides. Advanced Synthesis and Catalysis, 2012, 354, 1685-1691.	4.3	101
7	Pd-catalyzed aerobic oxidative coupling of anilides with olefins through regioselective C–H bond activation. Tetrahedron Letters, 2007, 48, 5449-5453.	1.4	96
8	Copper atalyzed Reductive Crossâ€Coupling of Nonactivated Alkyl Tosylates and Mesylates with Alkyl and Aryl Bromides. Chemistry - A European Journal, 2014, 20, 15334-15338.	3.3	95
9	Cu-Catalyzed Carbon-Heteroatom Coupling Reactions under Mild Conditions Promoted by Resin-Bound Organic Ionic Bases. Journal of Organic Chemistry, 2011, 76, 800-810.	3.2	73
10	Fluorescent recognition of uranyl ions by a phosphorylated cyclic peptide. Chemical Communications, 2015, 51, 11769-11772.	4.1	49
11	Construction of covalent organic framework with unique double-ring pore for size-matching adsorption of uranium. Nanoscale, 2020, 12, 24044-24053.	5.6	47
12	Cu-Catalyzed cross-coupling reactions of epoxides with organoboron compounds. Chemical Communications, 2015, 51, 2388-2391.	4.1	36
13	Efficient capture of actinides from strong acidic solution by hafnium phosphonate frameworks with excellent acid resistance and radiolytic stability. Chemical Engineering Journal, 2019, 355, 159-169.	12.7	33
14	Selective separation of thorium from rare earths and uranium in acidic solutions by phosphorodiamidate-functionalized silica. Chemical Engineering Journal, 2020, 392, 123717.	12.7	31
15	The preparation of organophosphorus ligand-modified SBA-15 for effective adsorption of Congo red and Reactive red 2. RSC Advances, 2019, 9, 13476-13485.	3.6	23
16	A category of hierarchically porous tin (IV) phosphonate backbone with the implication for radioanalytical separation. Chemical Engineering Journal, 2016, 302, 368-376.	12.7	22
17	Pore Size Control <i>via</i> Multiple-Site Alkylation to Homogenize Sub-Nanoporous Covalent Organic Frameworks for Efficient Sieving of Xenon/Krypton. ACS Applied Materials & Interfaces, 2021, 13, 1127-1134.	8.0	22
18	Pore Size Reduction by Methyl Function in Aluminum-Based Metal–Organic Frameworks for Xenon/Krypton Separation. Crystal Growth and Design, 2020, 20, 8039-8046.	3.0	21

CHU-TING YANG

#	Article	IF	CITATIONS
19	Novel polyazamacrocyclic receptor impregnated macroporous polymeric resins for highly efficient capture of palladium from nitric acid media. Separation and Purification Technology, 2020, 233, 115953.	7.9	19
20	Fabrication of a Li 4 SiO 4 –Pb tritium breeding material. Fusion Engineering and Design, 2014, 89, 3046-3053.	1.9	18
21	"One-pot―synthesis of amidoxime via Pd-catalyzed cyanation and amidoximation. Organic and Biomolecular Chemistry, 2015, 13, 2541-2545.	2.8	17
22	Density functional theory investigations on the binding modes of amidoximes with uranyl ions. Dalton Transactions, 2016, 45, 3120-3129.	3.3	16
23	Highly selective extraction of uranium from wastewater using amine-bridged diacetamide-functionalized silica. Journal of Hazardous Materials, 2022, 435, 129022.	12.4	15
24	Exploring the ability of triple quadrupole inductively coupled plasma mass spectrometry for the determination of Pu isotopes in environmental samples. Journal of Analytical Atomic Spectrometry, 2021, 36, 2330-2337.	3.0	13
25	The coordination of amidoxime ligands with uranyl in the gas phase: a mass spectrometry and DFT study. Dalton Transactions, 2016, 45, 16413-16421.	3.3	10
26	An initial demonstration of hierarchically porous niobium alkylphosphonates coordination polymers as potent radioanalytical separation materials. Journal of Chromatography A, 2017, 1504, 35-45.	3.7	10
27	The enhanced uranyl–amidoxime binding by the electron-donating substituents. RSC Advances, 2017, 7, 18639-18642.	3.6	9
28	Pdâ€Catalyzed Vinylation of Aryl Halides with Inexpensive Organosilicon Reagents Under Mild Conditions. Chemistry - A European Journal, 2018, 24, 10324-10328.	3.3	8
29	Efficient Synthesis of 1,5-Disubstituted Carbohydrazones Using K2CO3 As a Carbonyl Donor. Organic Letters, 2014, 16, 2398-2401.	4.6	7
30	Separation of minor actinides from highly acidic solutions using diglycolamide modified mesoporous silica synthesized via a novel "ring-opening click―reaction. Chemical Engineering Journal, 2022, 436, 135213.	12.7	7
31	Automated method for concurrent determination of thorium (²³⁰ Th, ²³² Th) and uranium (²³⁴ U, ²³⁵ U, ²³⁸ U) isotopes in water matrices with ICP-MS/MS. Journal of Analytical Atomic Spectrometry, 2022, 37, 919-928.	3.0	7
32	Promising density functional theory methods for predicting the structures of uranyl complexes. RSC Advances, 2014, 4, 50261-50270.	3.6	6
33	Stereocontrolled C(sp3)–P bond formation with non-activated alkyl halides and tosylates. RSC Advances, 2017, 7, 24652-24656.	3.6	6
34	Determination of trace rare earth elements in uranium ore samples by triple quadrupole inductively coupled plasma mass spectrometry. Journal of Analytical Atomic Spectrometry, 2021, 36, 2144-2152.	3.0	6
35	Radioanalytical chemistry for nuclear forensics in China: Progress and future perspective. Chinese Chemical Letters, 2022, 33, 3384-3394.	9.0	6
36	Binding affinity of pyridines with Am ^{III} /Cm ^{III} elucidated by density functional theory calculations. Dalton Transactions, 2019, 48, 1613-1623.	3.3	5

CHU-TING YANG

#	Article	IF	CITATIONS
37	The Hydrolytic Stability and Degradation Mechanism of a Hierarchically Porous Metal Alkylphosphonate Framework. Nanomaterials, 2018, 8, 166.	4.1	4
38	Cerium separation with NaBiO ₃ nanoflower material <i>via</i> an oxidation adsorption strategy. Journal of Materials Chemistry A, 2020, 8, 7907-7913.	10.3	4
39	Metal phosphonate sorbents: Enhancement of actinide sorption performance by gamma irradiation. Chemical Engineering Journal, 2021, 430, 132753.	12.7	4
40	Eliminating Mo isobaric interference using O ₂ as reaction gas for Tc measurement by triple quadrupole ICP-MS. Journal of Analytical Atomic Spectrometry, 2022, 37, 1174-1178.	3.0	3
41	Density Functional Theory Investigations on the Mechanism of Formation of Pa(V) Ion in Hydrous Solutions. Molecules, 2019, 24, 1169.	3.8	1
42	Density functional theory investigations on the coordination of Pa(v) with N,N-dialkylamide. New Journal of Chemistry, 2020, 44, 9477-9484.	2.8	1
43	The self-assembled AgCd nanoclusters: A novel plutonium separating material. Chemical Engineering Journal, 2022, 431, 134169.	12.7	1
44	A simple method for Ce–Nd separation using nano-NaBiO3: Application in the isotopic analysis of U, Sr, Pb, Nd, and Hf in uranium ores. Talanta, 2022, 245, 123443.	5.5	1
45	Investigating the performance of a Rh metal catalyst in hydrogen–deuterium exchange reactions in methane for application in low-temperature membrane separators. Fusion Engineering and Design, 2014, 89, 2666-2671.	1.9	0